

Research on Unlocking Force Characteristics of Landing Gear Finger Lock

ZHOU Fuliang^{1,2}, HOU Yu³, ZHANG Ming¹, NIE Hong^{2*}

1. State Key Laboratory of Mechanics and Control of Mechanical Structures, Nanjing University of Aeronautics and Astronautics, Nanjing 210016, P. R. China;
2. Key Laboratory of Fundamental Science for National Defense-Advanced Design Technology of Flight Vehicle, Nanjing University of Aeronautics and Astronautics, Nanjing 210016, P. R. China;
3. School of Aeronautic Engineering, Nanjing Vocational University of Industry Technology, Nanjing 210023, P. R. China

(Received 15 June 2022; revised 20 July 2023; accepted 20 September 2023)

Abstract: The influence of the length, diameter and fingertip angle of the finger lock on the unlocking force is studied, the theoretical calculation formula of the unlocking force is obtained, and the sensitivity of parameters to the unlocking force is analyzed. Firstly, the change law of the unlocking force is obtained by theoretical calculation. Then, the validity of the model is verified by experiments. Finally, the sensitivity of each parameter to the unlocking force is analyzed by orthogonal experiment. The result shows that the theoretical calculation formula is effective and reliable, the length, diameter 1 and diameter 2 of the finger lock are negatively correlated with the unlocking force, while the fingertip angle is positively correlated with the unlocking force; and the sensitivity of parameters affecting the unlocking force from high to low is finger lock length, diameter 1, fingertip angle and diameter 2.

Key words: landing gear; finger lock; sensitive parameter; orthogonal experiment; force analysis

CLC number: V226 **Document code:** A **Article ID:** 1005-1120(2024)01-0088-09

0 Introduction

Landing gear is an important mechanism for aircraft taking off and landing. When the landing gear is retracted and extended, the locking mechanism^[1] will complete the locking to fix the landing gear, so that the aircraft can take off and land safely. Therefore, whether the landing gear lock mechanism can work normally is directly related to the safety of aircraft taking off and landing^[2], which is an important part of landing gear design. During the use of aircraft landing gear, the unlocking force of lock mechanism is variable in the process of unlocking and locking^[3]. If the unlocking force is abnormal, it will lead to landing gear retraction failure and threaten the safety of aircraft taking off and landing^[4-5].

Many researches have been done on the param-

eter design and parameter sensitivity of landing gear at home and abroad^[6-7]. Bagrov et al.^[8] studied landing mechanical properties of landing gear under fixed design parameters. In Ref.[9], Ding et al. studied the sensitive factors of landing gear during landing, and optimized the design parameters of landing gear. In contact theory, Hertz contact^[10] and Coulomb friction theorem^[11] were often used to calculate the friction. Lu et al.^[12] studied the structural parameters of the main shaft in the mine hoisting system on the device reliability. Li et al.^[13] carried out parameter sensitivity analysis on socket in aerospace equipment. Barsoum et al.^[14] obtained the sensitive parameters of double notched tube (DNT) failure by experimental method. However, there is no sensitivity analysis on the geometric parameters of finger lock.

*Corresponding author, E-mail address: hnie@nuaa.edu.cn.

How to cite this article: ZHOU Fuliang, HOU Yu, ZHANG Ming, et al. Research on unlocking force characteristics of landing gear finger lock[J]. Transactions of Nanjing University of Aeronautics and Astronautics, 2024, 41(1):88-96.

<http://dx.doi.org/10.16356/j.1005-1120.2024.01.007>

In the actual working process, it can be found that the unlocking force of the finger lock will change in a complete working cycle, which will affect the stability of landing gear retraction and extension, and even block in serious cases. Therefore, it is necessary to study the sensitivity of each design parameter to the unlocking force and the changing law of the unlocking force. In this paper, the influence of different parameters (the length L , diameters Φ_1 and Φ_2 , fingertip angle θ) on the unlocking force of landing gear actuating cylinder is studied. The mechanical characteristics of the release process of the finger lock are analyzed theoretically, the release process of the finger lock in the real landing gear retraction process is simulated by experiments, and the correctness of the theoretical calculation is verified. Finally, using the method of orthogonal experiment, the sensitivity of each parameter to the unlocking force is obtained, which provides the basis for the finger lock design.

1 Mechanical Model of Finger Lock

1.1 Introduction of finger lock

The landing gear retracts or deploys during takeoff or landing. In order to make the aircraft safe, it is necessary to use the locking mechanism to lock the retractable landing gear. The lower position lock is often used in the folding landing gear. When the landing gear changes from folded to unfolded before landing, a lower position lock is needed to lock the landing gear to maintain its stable starting state. Finger lock is a kind of lower lock, which is stable and reliable and can bear large load. This kind of lock mechanism is shown in Fig.1(a). The process of unlocking and locking the finger lock needs to be completed with the assistance of relevant auxiliary agencies. The main design parameters of the finger lock studied in this paper are shown in Fig.1(b). The bulge at the bottom of the finger lock matches the groove on the corresponding base. Among them, the sensitive parameters studied are the length L , diameters Φ_1 and Φ_2 , and fingertip angle θ .

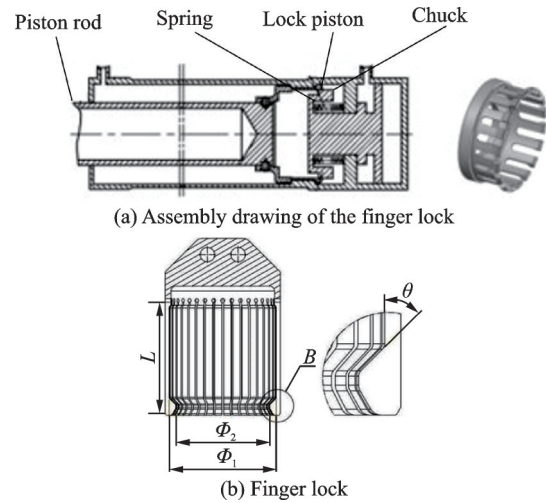


Fig.1 Illustration of finger locks

1.2 Mechanical model of finger lock/unlocking process

The working process of finger lock is divided into two parts: Unlocking process and locking process.

During the unlocking process, the finger lock is subjected to the axial force P_1 . In this process, the finger lock overcomes friction force f_1 produced by the normal force N_1 and moves upward, moves 40 mm and stops to complete the unlocking process, as shown in Fig.2.

During the locking process, the finger lock is subjected to the axial force P_2 . The finger lock is

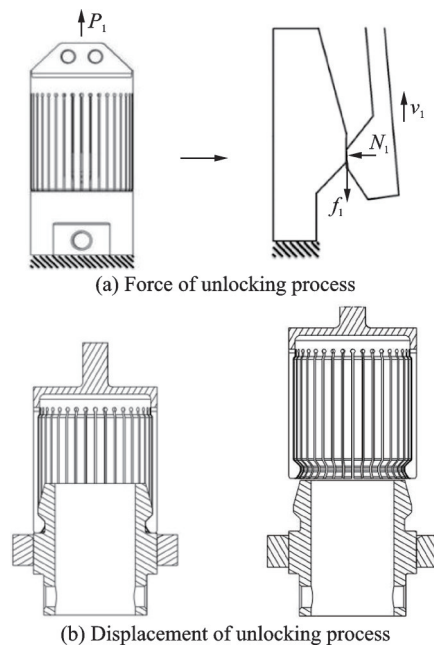


Fig.2 Force and displacement of unlocking process

squeezed by the base boss and opens radially. After crossing the boss, it is closed again and stuck in the slot of the base. In this process, the finger lock overcomes friction force f_2 produced by the normal force N_2 and moves down, moves 40 mm, just returns to the initial position and completes the locking process, as shown in Fig.3.

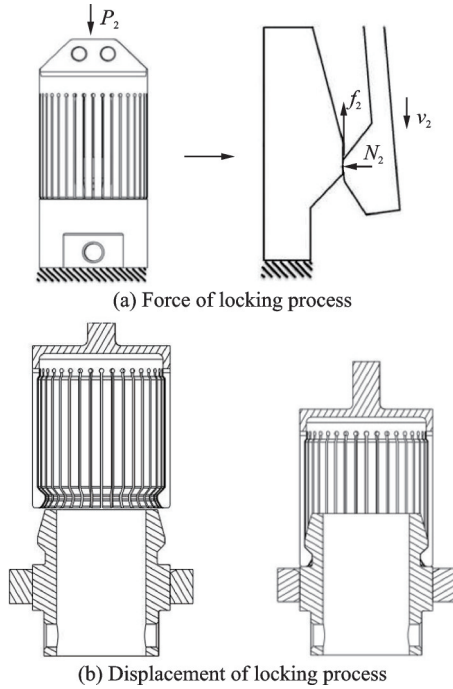


Fig.3 Force and displacement of locking process

In the unlocking process, the finger lock is opened by the base, and the single finger of the lock is in a pure bending state. In Fig.4, it is the geometric position of the finger lock that produces the maximum bending.

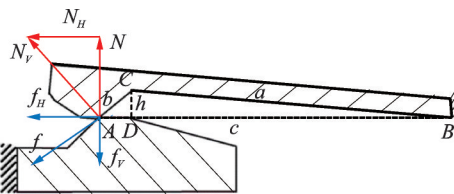


Fig.4 Force analysis of finger lock during unlocking

As shown in Fig.4, the edges AB , BC and AC are represented as c , a and b , respectively; the length of CD is h ; the angles at A , B and C are α , β and γ , respectively. The relationship between γ and θ is $\gamma + \theta = \pi$.

According to the geometric relation of triangle,

sine theorem and cosine theorem, the result can be obtained as

$$\cos \gamma = \frac{a^2 + b^2 - c^2}{2ab} \quad (1)$$

$$\sin \alpha = \frac{h}{b} \quad (2)$$

$$\sin \beta = \frac{h}{a} \quad (3)$$

$$\frac{\sin \alpha}{a} = \frac{\sin \beta}{b} = \frac{\sin \gamma}{c} \quad (4)$$

By solving Eqs.(1–4), the deflection at C can be obtained as

$$h = \frac{a^2 \sin \gamma \cos \gamma + \sqrt{a^2 c^2 \sin^2 \gamma - a^4 \sin^4 \gamma}}{c} \quad (5)$$

Among them

$$\gamma = \pi - \theta \quad (6)$$

According to the proportional relation, the deflection at A can be obtained as

$$h_A = \frac{c}{a} h = a \sin \gamma \cos \gamma + \sqrt{c^2 \sin^2 \gamma - a^2 \sin^4 \gamma} = \sqrt{c^2 \sin^2 \theta - a^2 \sin^4 \theta} - a \sin \theta \cos \theta \quad (7)$$

Fig.5 shows the relationship of h_A , c and θ . It can be seen that in the value range of 117–140 mm, the value of h_A increases with the increase of c . In this value range, they are positively correlated. In the range of 0° to 90° , the values of h_A increase with the increase of θ , and they are positively correlated.

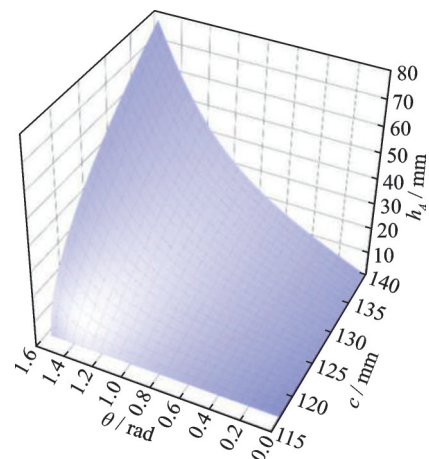


Fig.5 Relationship of h_A , c and θ

According to the deflection equation, the pressure N at A can be obtained as

$$N = \frac{3h_A EI}{c^3} \quad (8)$$

After introducing the relevant parameters into

Eq.(8), the pressure N is

$$N = \frac{3EI \left(a \sin \gamma \cos \gamma + \sqrt{c^2 \sin^2 \gamma - a^2 \sin^4 \gamma} \right)}{c^3} = \frac{3EI \left(\sqrt{c^2 \sin^2 \theta - a^2 \sin^4 \theta} - a \sin \theta \cos \theta \right)}{c^3} \quad (9)$$

It can be seen from Fig.4 that the total pressure N is vertical downward. Therefore, the pressure N_v perpendicular to edge AC and force component N_H in AB horizontal direction at point A are

$$N_v = \frac{N}{\cos \alpha} = \frac{3EI \left(\sqrt{c^2 \sin^2 \theta - a^2 \sin^4 \theta} - a \sin \theta \cos \theta \right)}{c^3 \cos \alpha} \quad (10)$$

$$N_H = N \cdot \tan \alpha = \frac{3EI \tan \alpha \left(\sqrt{c^2 \sin^2 \theta - a^2 \sin^4 \theta} - a \sin \theta \cos \theta \right)}{c^3} \quad (11)$$

Among them

$$\cos \alpha = \sqrt{1 - \left(\frac{h}{b} \right)^2} = \sqrt{1 - \left(\frac{\sqrt{a^2 c^2 \sin^2 \theta - a^4 \sin^4 \theta} - a^2 \sin \theta \cos \theta}{c \sqrt{c^2 - a^2 \sin^2 \theta} - ca \cos \theta} \right)^2} \quad (12)$$

$$\tan \alpha = \frac{h}{\sqrt{b^2 - h^2}} = \frac{1}{\sqrt{\left(\frac{b}{h} \right)^2 - 1}} = \frac{1}{\sqrt{\left(\frac{c \sqrt{c^2 - a^2 \sin^2 \theta} - ca \cos \theta}{\sqrt{a^2 c^2 \sin^2 \theta - a^4 \sin^4 \theta} - a^2 \sin \theta \cos \theta} \right)^2 - 1}} \quad (13)$$

In the edge AC , there is friction force f . After decomposing f , their relationship is as follows

$$\begin{cases} f_H = f \cos \alpha \\ f = \mu N_v \end{cases} \quad (14)$$

After introducing the correlation equation, f_H can be obtained as

$$f_H = \mu N = \frac{3\mu EI \left(\sqrt{c^2 \sin^2 \theta - a^2 \sin^4 \theta} - a \sin \theta \cos \theta \right)}{c^3} \quad (15)$$

Therefore, the total unlocking force F is as follows

$$F = 36(N_H + f_H) = \frac{36 \times 3EI (\mu + \tan \alpha) \left(\sqrt{c^2 \sin^2 \theta - a^2 \sin^4 \theta} - a \sin \theta \cos \theta \right)}{c^3} \quad (16)$$

where the number of petals of finger lock is 36.

Fig.6 shows the relationship of F , c and θ . It can be seen from Fig.6 that in the range of 117—140 mm, the value of F increases with the increase of c , showing a positive correlation in this value range. In the range of 0° to 90° , the value of F increases with the increase of θ , showing a positive correlation.

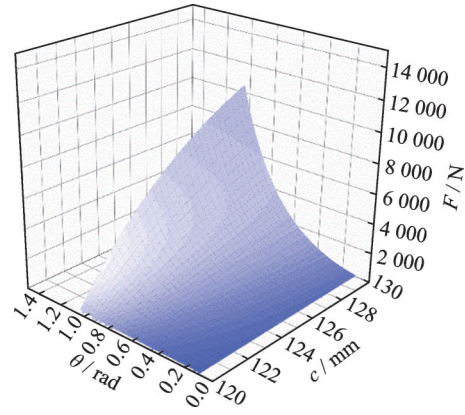


Fig.6 Relationship of F , c and θ

2 Experimental Verification of Mechanical Calculation Model of Finger Lock

The finger lock experiment is carried out on an electric testing machine. During the experiment, the upper and lower bases are connected with the upper and lower loading ends of the loading equipment by bolts, respectively. The upper base is movable and the lower one is fixed. The SANS electronic tester and data acquisition control interface diagram are shown in Fig.7. The assembly diagram of finger lock in the experiment is shown in Fig.8.

As shown in Fig.9, nine types of finger locks are carried out in the experiment. The specific design parameters of finger locks are shown in Table 1. Among them, the reference type is 001.

Finally, the unlocking force curves of finger lock with different design parameters are obtained.

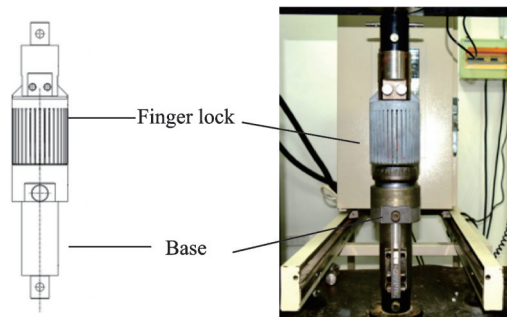


(a) The SANS electronic experimental machine



(b) The control interface

Fig.7 The SANS electronic experimental machine and its data acquisition control interface



(a) CAD assembly

(b) Test specimen

Fig.8 Finger lock in experiment



Fig.9 Physical pictures of nine types of finger locks

As shown in Fig.10, the abscissa represents the displacement of the finger lock; the ordinate represents the release force of the finger lock; the tensile force is positive and the compression force is negative.

Table 1 Design parameters for each finger lock

Serial number	Type	$L/$ mm	$\Phi_1/$ mm	$\Phi_2/$ mm	$\theta/$ (°)	Maximum un- locking force/ N
1	001	120	111.6	98	45	3 960
2	009	90	111.6	98	45	9 828
3	011	140	111.6	98	45	2 376
4	013	120	113.6	98	45	2 042
5	015	120	112.6	102	45	2 033
6	017	120	111.6	102	45	2 803
7	021	120	111.6	98	60	6 724
8	023	120	113.6	98	60	3 202
9	025	90	111.6	98	60	15 869

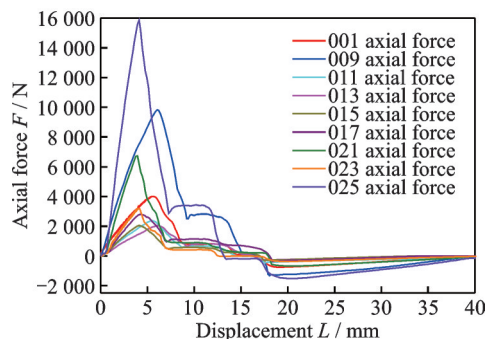


Fig.10 Variation of the axial force with displacement for nine types of finger locks

The unlocking process of finger lock is obviously divided into four curves, namely phase 1, phase 2, phase 3 and phase 4, as shown in Fig.11.

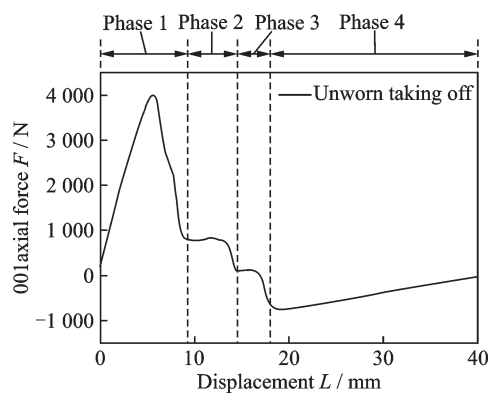


Fig.11 Variation of 001 axial force with displacement

At phase 1, the axial force increases rapidly and reaches the maximum value during the separation process. The axial force is tensile force, and the value is positive. At phase 2, the axial force decreases and maintains a constant value. The axial force is still tension. At phase 3, due to the springback

trend of elastic deformation, the axial force required will continue to decrease and maintain at a constant value in this process. However, friction is the main source at this time, so the process is still to overcome friction. Therefore, the axial force is still tension, and the value is positive. At phase 4, since the elastic rebound begins, the component force generated by the rebound is far greater than that provided by the friction force. Therefore, the axial force in this process is pressure, and the value is negative. The axial force reaches the minimum value in unlocking process, and the absolute value gradually decreases until it is zero.

Table 2 shows the comparison between the experimental and calculated results for nine finger locks. From Table 2, it can be seen that the calculation results are consistent with the experimental results, which can comparatively accurately predict the mechanical behavior of finger lock.

Table 2 Comparison between experimental and calculation results for nine finger locks

Serial number	Type number	Maximum experimental unlocking force /N	Maximum calculation unlocking force/N
1	001	3 960	3 752
2	009	9 828	8 137
3	011	2 376	2 456
4	013	2 042	1 740
5	015	2 033	2 239
6	017	2 803	3 343
7	021	6 724	7 302
8	023	3 202	3 080
9	025	15 869	15 785

3 Sensitivity Analysis of Finger Lock Parameters

According to the effective theoretical calculation model of finger locks, the unlocking force with different parameters can be obtained. According to the results of theoretical calculation, the change law of unlocking force and the sensitive parameters affecting the unlocking force of finger lock are compared and analyzed.

The orthogonal experiment method is an experimental design method that uses orthogonal table to

select representative combinations from all test combinations, then process and analyze these experimental data to obtain the most appropriate combination. The structural design parameters of finger lock studied in this paper are shown in Fig.1(b) and Table 3.

Table 3 Initial structure parameters of finger lock

L/mm	Φ_1/mm	Φ_2/mm	$\theta/(\text{°})$
120	111.6	98	45

L , Φ_1 , Φ_2 and θ are taken as experimental factors. Subsequently, the base value of L is taken as 120 mm with every 20 mm as a factor, the base value of Φ_1 is taken as 111.6 mm with every 1 mm as a factor, the base value of Φ_2 is taken as 98 mm with every 2 mm as a factor, the base value of θ is taken as 45° with every 5° as a factor. An orthogonal experimental design with 4 factors and 5 levels can be obtained, as shown in Table 4.

Table 4 Orthogonal experimental design of finger lock

Level	Factor			
	L/mm	Φ_1/mm	Φ_2/mm	$\theta/(\text{°})$
1	80	109.6	94	40
2	100	110.6	96	45
3	120	111.6	98	50
4	140	112.6	100	55
5	160	113.6	102	60

According to the experimental scheme shown in Table 4, the total number of experiments with 4 factors and 5 levels is 5^4 groups, which is very large and cannot be tested one by one in production practice and scientific research. However, with the method of orthogonal experimental method, only 25 groups of experiments are needed to obtain the optimal combination scheme. The properties of orthogonal table are known as: (1) The number of different numbers in each column is equal; (2) In any two columns, when two numbers in the same row are regarded as ordinal pairs, the number of occurrences of each pair is equal. Using the properties, the L25 orthogonal experimental table can be created. Taking the data of Table 4 into L25 orthogonal experimental table, the results of mechanical analysis of the model can be obtained as shown in Table 5.

Table 5 Orthogonal experiment of finger lock and its results

Experiment serial number	Variable parameter				Maximum axial unlocking force /N
	L/mm	Φ_1/mm	Φ_2/mm	$\theta/(\circ)$	
1	80	109.6	94	40	18 857
2	80	110.6	96	45	17 090
3	80	111.6	98	50	14 710
4	80	112.6	100	55	11 955
5	80	113.6	102	60	9 069
6	100	109.6	98	45	12 001
7	100	110.6	100	50	10 523
8	100	111.6	102	55	8 755
9	100	112.6	94	60	11 228
10	100	113.6	96	40	2 117
11	120	109.6	102	50	7 651
12	120	110.6	94	55	11 293
13	120	111.6	96	60	9 928
14	120	112.6	98	40	1 867
15	120	113.6	100	45	1 410
16	140	109.6	96	55	9 572
17	140	110.6	98	60	8 668
18	140	111.6	100	40	1 610
19	140	112.6	102	45	1 258
20	140	113.6	94	50	1 668
21	160	109.6	100	60	7 429
22	160	110.6	102	40	1 347
23	160	111.6	94	45	2 055
24	160	112.6	96	50	1 696
25	160	113.6	98	55	1 309

According to the analysis results in Table 5. The mean, range and variance of experimental results corresponding to each level of finger lock geometric parameters are calculated. Then the orthogonal experimental analysis can be obtained as shown in Table 6.

Table 6 Orthogonal experiment analysis of finger lock

Average of level	L/mm	Φ_1/mm	Φ_2/mm	$\theta/(\circ)$
$T1$	14.3e+03	11.1e+03	9.02e+03	5.16e+03
$T2$	8.92e+03	9.78e+03	8.08e+03	6.76e+03
$T3$	6.43e+03	7.41e+03	7.71e+03	7.25e+03
$T4$	4.56e+03	5.60e+03	6.59e+03	8.58e+03
$T5$	2.77e+03	3.11e+03	5.62e+03	9.26e+03
R	11.6e+03	7.99e+03	3.40e+03	4.10e+03
S	20.2e+06	10.2e+06	1.76e+06	2.58e+06

In Table 6, $T1$, $T2$, $T3$, $T4$ and $T5$ represent the average maximum axial unlocking force of the finger lock in level 1, level 2, level 3, level 4 and

level 5 (in Table 4) according to the calculation results of each factor in Table 5, respectively. The influence of the horizontal variation of each factor on the maximum axial unlocking force is reflected by the range R under each level of the same factor. The significant difference of the maximum axial unlocking force caused by the level change of each factor is evaluated by the variance S under each level of the same factor. The larger the range R and variance S are, the greater the influence of the horizontal variation of the geometric parameter on the maximum axial unlocking force is, and the more significant and the higher the sensitivity is.

According to Table 6, the results of range analysis and variance analysis are consistent. The sensitivity of the finger lock geometric parameters to the maximum axial unlocking force from high to low is L , Φ_1 , θ and Φ_2 . The influence curves of geometric parameters of finger lock are as shown in Fig.12. It

can be seen from Fig.12 that L , Φ_1 and Φ_2 are negatively correlated with the unlocking force, and θ is positively correlated with the unlocking force.

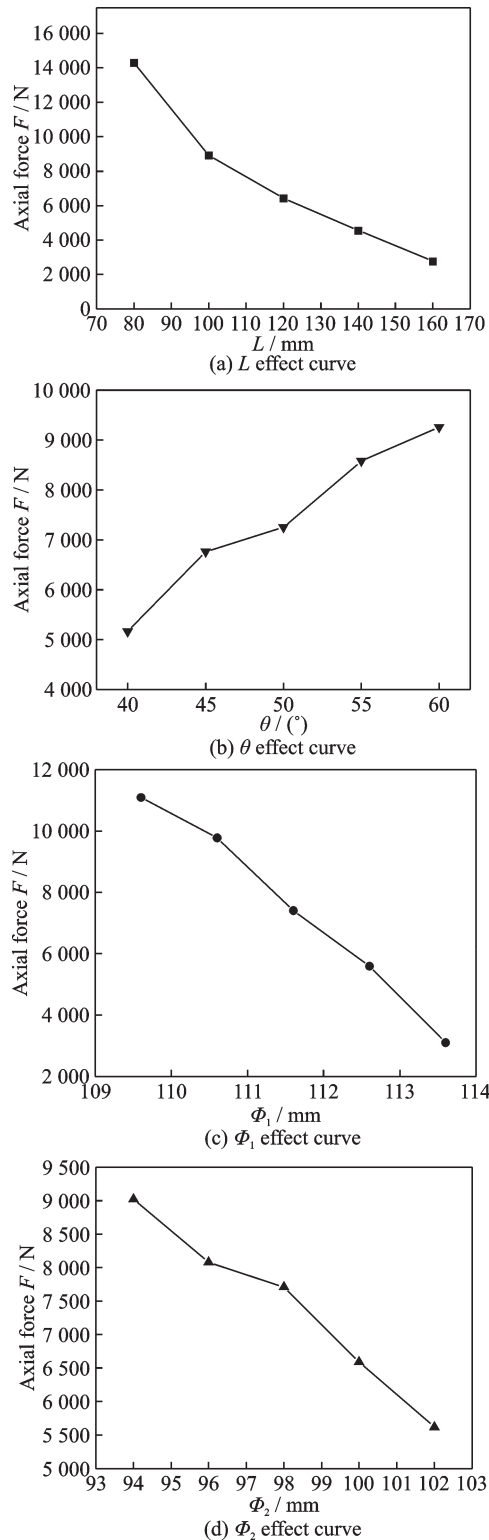


Fig.12 Parameter effect curves of finger lock

4 Conclusions

The relationship among different geometric pa-

rameters (L , Φ_1 , Φ_2 , θ) and the unlocking force of the finger lock in the landing gear actuator are studied. The theoretical calculation, experimental verification and parameter sensitivity analysis of the locking force are carried out, and the following conclusions can be drawn.

(1) Finger lock length L , diameters Φ_1 and Φ_2 have a negative correlation with the maximum unlocking force F ; θ has a positive correlation with the maximum unlocking force F .

(2) The unlocking process of finger lock is obviously divided into four sections. In phase 1 unlocking force reaches the maximum value, and the axial force is tensile force. In phase 2, the axial force will decrease and maintain a relatively constant value, and the axial force is still tensile force. In phase 3, friction is the main source, and the axial force is still tension. In phase 4, the axial force is the pressure, and the axial force reaches the minimum value.

(3) According to the results of the orthogonal experiment, it can be seen that the sensitivity of the geometric parameters of the finger lock to the maximum axial unlocking force from high to low is L , Φ_1 , θ and Φ_2 . Among them, L and Φ_1 are high sensitive parameters, while θ and Φ_2 are less sensitive.

References

- [1] CURREY N S. Aircraft landing gear design: Principles and practices[M]. [S.l.]: American Institute of Aeronautics and Astronautics, 1988.
- [2] BAGNOLI F, DOLCE F, COLAVITA M, et al. Fatigue fracture of a main landing gear swinging lever in a civil aircraft[J]. Engineering Failure Analysis, 2008, 15(6): 755-765.
- [3] MOFIDI M, PRAKASH B. Two body abrasive wear and frictional characteristics of sealing elastomers under unidirectional lubricated sliding conditions[J]. Tribology Materials, 2010, 4(1): 26-37.
- [4] OSSA E A. Failure analysis of a civil aircraft landing gear[J]. Engineering Failure Analysis, 2006, 13(7): 1177-1183.
- [5] KAUZLARICH J J, WILLIAMS J A. Archard wear and component geometry[J]. Proceedings of the Institution of Mechanical Engineers, Part J: Journal of Engineering Tribology, 2001, 215(4): 387-403.
- [6] VIET L Q, HWANG J H. A semi-active controller for an aircraft landing gear equipped with magnetorheo-

- logical damper[J]. Applied Mechanics and Materials, 2019, 894: 29-33.
- [7] VECHTEL D. How future aircraft can benefit from a steerable main landing gear for crosswind operations[J]. CEAS Aeronautical Journal, 2020, 11(2): 417-429.
- [8] BAGROV K V. Numerical simulation of planar oscillations of a landing gear leg along the longitudinal axis of an aircraft during the landing impact[J]. Journal of Applied and Industrial Mathematics, 2019, 13(3): 385-389.
- [9] DING Zongmao, WU Hongyu, WANG Chunjie, et al. Hierarchical optimization of landing performance for lander with adaptive landing gear[J]. Chinese Journal of Mechanical Engineering, 2019, 32(2): 24-35.
- [10] ZHAO K, OKOLO P, NERI E, et al. Noise reduction technologies for aircraft landing gear—A bibliographic review[J]. Progress in Aerospace Sciences, 2020, 112: 100589.
- [11] TUCKER S, ADAM D, QUINTON M, et al. Ion friction at small values of the Coulomb logarithm[J]. Physical Review E Statistical Physics Plasmas Fluids & Related Interdisciplinary Topics, 2019, 99(5): 53206.
- [12] LU Hao, PENG Yuxing, SHUANG Chao, et al. Parameter sensitivity analysis and probabilistic optimal design for the main-shaft device of a mine hoist[J]. Arabian Journal for Science and Engineering, 2019, 44(2): 971-979.
- [13] LI Cuiling, DAI Pengfei, YANG Qiang, et al. Contact performance evaluation and parameter sensitivity analysis for aerospace electrical connector[J]. Journal of Northeastern University, 2018, 39(1): 71-75.
- [14] BARSOUM I, AL-KHALED M. The sensitivity to the lode parameter in ductile failure of pressure vessel tubular steel grades[J]. Journal of Pressure Vessel Technology, 2018, 140(3): 031402.

Acknowledgement This work was supported by the Fundamental Research Funds for the Central Universities (No. NS2019003).

Authors Mr. ZHOU Fuliang received the M.S. degree in Aircraft Design and Engineering from Nanjing University of Aeronautics and Astronautics (NUAA) in 2008, and he is now a Ph.D. candidate in Aircraft Design from NUAA. His current research interests include aircraft design and landing gear system.

Prof. NIE Hong received the Ph.D. degree in Aircraft Design from NUAA in 1992. Now he is a professor in NUAA. His current research interests include aircraft design, dynamics and landing gear system.

Author contributions Prof. NIE Hong designed the study and raised the idea. Mr. ZHOU Fuliang assisted in writing the manuscript. Prof. ZHANG Ming and Dr. HOU Yu contributed to the data for the analysis, the discussion and background of the study. All authors commented on the manuscript draft and approved the submission.

Competing interests The authors declare no competing interests.

(Production Editor: WANG Jing)

起落架指型锁解锁力特性的研究

周福亮^{1,2}, 侯 聿³, 张 明¹, 聂 宏²

(1. 南京航空航天大学机械结构力学及控制国家重点实验室, 南京 210016, 中国;

2. 南京航空航天大学飞行器先进设计技术国防重点学科实验室, 南京 210016, 中国;

3. 南京工业职业技术大学航空工程学院, 南京 210023, 中国)

摘要: 研究了指型锁的长度、直径和指尖角度等因素对解锁力的影响, 获得了解锁力的理论计算公式并分析了影响解锁力的敏感参数。首先对指型锁解锁力进行理论计算, 获得解锁力与各个参数变化的变化规律; 然后通过实验验证模型的有效性; 最后使用正交实验法分析了各参数对解锁力影响的敏感性。结果表明, 本文所得计算公式有效可靠; 指型锁长度、直径1、直径2与解锁力负相关, 指尖角度与解锁力正相关; 影响解锁力的参数敏感性由高到低分别为指型锁长度、直径1、指尖角度和直径2。

关键词: 起落架; 指型锁; 敏感参数; 正交试验; 力分析